Smart Structures and Systems, *Vol. 27, No. 4 (2021) 641-650*
DOI: https://doi.org/10.12989/sss.2021.27.4.641

Energy harvesting of sandwich beam with laminated composite core and piezoelectric face sheets under external fluid flow

Ali Ghorbanpour Arani*[1,2], Ashkan Farazin [1], Mehdi Mohammadimehr [1] and Shahram Lenjannejadian [3]

[1] *Department of Solid Mechanics, Faculty of Mechanical Engineering, University of Kashan, Kashan, Iran P.O. Box 87317-53153*
[2] *Institute of Nanoscience & Nanotechnology, University of Kashan, Kashan 87317-53153, Iran*
[3] *Department of Sport Biomechanics, Faculty of Sport Sciences, University of Isfahan, Isfahan, Iran*

(*Received April 7, 2020, Revised September 23, 2020, Accepted December 19, 2020*)

Abstract. In the present study, the generation of electrical energy from induced vibrations in a composite beam with piezoelectric layer are studied. Accordingly, using Euler-Bernoulli beam theory and considering two types of air damping (external damping) and structural damping (internal damping), the equations of motion for sandwich beam are obtained and then using the Kantorovich method, the output voltage relations for a composite beam with a piezoelectric layer are extracted. After validating the analytical results with the results in the literature, the effect of various parameters such as external fluid flow rate, fiber angle, and how the piezoelectric layer composite beams are arranged on energy harvesting. Also, the maximum oscillation amplitude are investigated. The results show that by using composite materials and with proper layer design and fiber angle in each layer, a different equivalent modulus of elasticity can be created in the composite beam, which will change the normal frequency of the system and the output voltage range of the circuit. The results show that the angle of the fibers has a significant effect on the damping coefficient of the structure, flexural stiffness, natural frequency and finally energy harvesting. According to the results, it can be seen that the minimum value of voltage per use of fibers with an angle of 50 degrees and the maximum amount of voltage per use of fibers with an angle of zero degrees are occurred.

Keywords: energy harvesting; sandwich beam; Kantorovich method; piezoelectric face sheets; Euler-Bernoulli beam theory

1. Introduction

Recently, the composite and sandwich structures such as carbon nanotubes (CNTs) have been considered as a novel generation of materials by researchers (Farazin and Mohammadimehr 2020, Khandan *et al*. 2020, Farazin *et al*. 2020). Today, the use of piezoelectric converters due to the ability to convert environmental energy such as mechanical vibrations into electrical energy has found wide application in many industries (Farazin *et al*. 2019). In a piezoelectric layer structure, in addition to the piezoelectric properties, the non-piezoelectric properties of the energy harvesting structure are also important. In recent years, there have been many studies on energy harvesting using various sources due to the need to supply low-power electronic circuits such as sensors and wireless systems (Trentadue *et al*. 2019, Hannan *et al*. 2018, Kim *et al*. 2010). Rajabi and Mohammadimehr (2019) considered bending analysis of a micro sandwich skew plate using extended Kantorovich method based on Eshelby-Mori-Tanaka approach. AkhavanAlavi *et al*. (2019) illustrated active control of micro Reddy beam integrated with functionally graded nanocomposite sensor and actuator based on linear quadratic regulator method. Energy harvesting is the process of extracting all kinds of environmental energy from the various methods (Cahill *et al*. 2018). No need to replace worn-out batteries, reduce maintenance costs from reviewing and replacing batteries for wireless networks, and using in-vivo medical devices are important reasons for using energy harvesters (Kim *et al*. 2016). Piezoelectric materials are a group of intelligent materials that convert mechanical strain to electrical voltage and also they have a higher power density than other energy-saving methods (Ghorbanpour Arani and Zamani 2018, Ghorbanpour Arani *et al*. 2019, Mohammadimehr *et al*. 2017, Soleymani and Ghorbanpour Arani (2019). Therefore, these materials are one of the main options in energy harvesting from vibrations and mechanical movements of the surrounding environment (Ghorbanpour Arani *et al*. 2017). Many researchers have investigated the use of piezoelectric materials for energy harvesting in mechanical structures, for example, Umeda *et al*. (1996) were among the first researchers in the field of energy harvesters. Their proposed model was a discrete model consisting of a mass, a spring, and damping. Li *et al*. (2011) investigated a small electrical generators with bent piezoelectric beam on elastic foundation. (Xie *et al*. 2012) harvested energy from a fluid flow using a flexible piezoelectric cylinder. They used a one-dimensional numerical model to simulate the proposed system. Their results show that using a cylinder with

*Corresponding author, Professor,
E-mail: aghorban@kashanu.ac.ir

ISSN: 1738-1584 (Print), 1738-1991 (Online)

dimensions of 1 cm in diameter and 40 cm in length at a flow rate of 5 m/s can produce about 103 watts of energy. Mohammadimehr *et al*. (2016) presented biaxial and shear nonlinear buckling analysis of nonlocal isotropic and orthotropic micro-plate based on surface stress and modified couple stress theories using differential quadrature methods. Using a theoretical model, Zhou *et al*. (2017) investigated the ability to harvest electrical energy in the microwave range from a zigzag beam with a ceramic piezoelectric layer. Then the results of the analytical solution were compared with the experimental results. Ottman *et al*. (2002) described a new approach to energy harvesting from piezoelectric materials. They used a capacitive circuit and a diode to rectify the output electrical voltage, and also optimized the maximum power output for wireless networks. Mohammadimehr *et al*. (2018) investigated bending, buckling, and free vibration analyses of carbon nanotube reinforced composite beams and experimental tensile test to obtain the mechanical properties of nanocomposite. An Tan *et al*. (2018) studied energy harvesting from an isotropic beam with a piezoelectric layer. In their analysis, they used a piezoelectric polymer field for energy harvesting and used the transfer function method to solve their equation. Using this method helped them to apply different forces such as massive load to stimulate the beam.

Shan *et al*. (2019) proposed a new piezoelectric energy harvester capable of operating in the water. Using empirical studies, they examined the performance of the new proposed system and they showed that the new proposed system could increase the output voltage up to 99% over conventional systems. In one of the most recent research in this field, Li *et al*. (2020) presented a piezoelectric multilayer energy harvester. They considered bimorph beam consisted of carbon and glass fibers as reinforcements. They studied energy harvesting of a new system using theoretical models and empirical and experimental tests. The results of their study showed that using the proposed new system can improve energy harvesting capability up to 2.5 times more than conventional energy harvesting models. Babaeeian and Mohammadimehr (2020) considered the time elapsed effect on residual stress measurement in a composite plate by DIC method.

A review of studies on energy harvesting shows that most previous research has focused on the harvesting of electrical energy from a metal alloy of cantilever beam which has isotropic properties. On the other hand, in recent years, composite materials or sandwich structures have been widely used in various industries due to their unique mechanical properties compared to isotropic materials. Since the energy harvesting by inductive vibration in the composite beam by fluid flow has not been studied so far, therefore, this paper studies the energy harvesting from a rectangular composite beam with two layers of piezoelectric under forced vibration induced by external fluid flow. For this purpose, the governing equations of motion for the composite beam with a piezoelectric layer under induction vibration induced by external fluid flow have been developed by considering structural and external damping, and finally, the influence of parameters affecting energy harvesting rates such as fluid flow rate, layout, angle fibers, and geometrical properties are examined.

2. Extraction of motion equations

In the present study, the energy harvesting of a composite bimorph beam is examined. The composite beam under investigation is a cantilever rectangular beam with a concentric mass at the end shown in Fig. 1. The beam with width "b" and length "L" consists of a multilayer of carbon/epoxy with the thickness of "h_s" as the core of the sandwich beam and two layers of "*PZT5A*" ceramic piezoelectric with the thickness of "h_p" as face sheets. Face sheets must be as energy harvester which affected by the flow induced by the fluid. Assuming thickness of beam is thin therefore, displacement fields can be expressed based on the Euler-Bernoulli beam theory. Accordingly, the transverse vibration behavior of the composite biomorphic beam with respect to mechanical and external forces due to the fluid can be expressed by Erturk and Inman (2011), Alsaadi *et al*. (2019) as follows

$$\frac{\partial^2 M(x,t)}{\partial x^2}+\frac{\partial^2}{\partial x^2}\left(C_s I\frac{\partial^3 w(x,t)}{\partial x^2 \partial t}\right)+C_a\frac{\partial w(x,t)}{\partial t} +(m+M_1\delta(x-L))\frac{\partial^2 w(x,t)}{\partial t^2}=f(x,t) \tag{1}$$

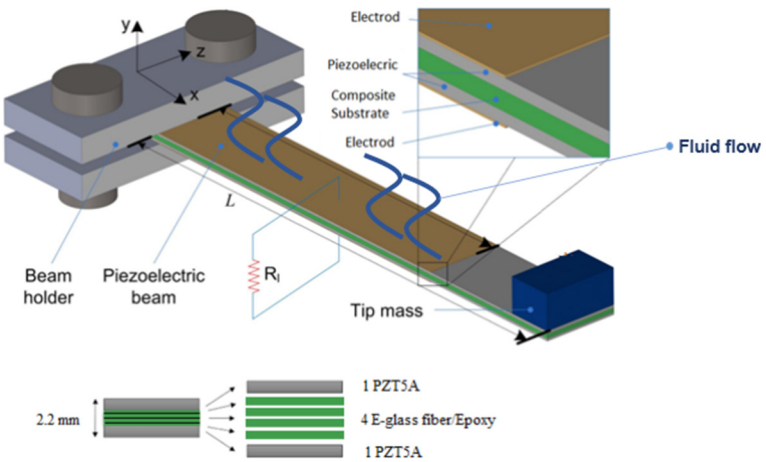

Fig. 1 Schematic model of a bimorph composite beam with two piezoelectric layers affected by external fluid flow

where "$w(x,t)$" is transverse beam displacement, "$M(x,t)$" is the bending moment of composite beam considering the effects of piezoelectric layers, "C_s" is the strain-rate damping coefficient (it appears as an effective term "C_sI" for the composite structure), "C_a" is the viscous air damping coefficient, "M_1" is concentrated mass and, "m" is mass of unit length of beam. The steps to prove Eq. (1) with detailed process is shown in Appendix A. It is worth mentioning in this paper, the direction of motion of the fluid is perpendicular to the axis of the beam, and because we were considering transverse vibration, the "y" direction is the direction of motion of the fluid flow.

In Eq. (1), the resulting torque depends on the internal stresses of the sandwich beam, which can be obtained as follows

$$\begin{aligned} M(x,t) &= -b\int_{t_L}\sigma_L z dz - b\int_{t_p}\sigma_p z dz \\ &= -b\sum_{k=1}^{N_c}\int_{t_{Lk}}\sigma_L z dz - b\sum_{k=1}^{N_p}\int_{t_{pk}}\sigma_p z dz \end{aligned} \tag{2}$$

where "σ_L"and "σ_p" shows the normal stresses of the composite and piezoelectric each layers, respectively that becomes based on the local coordinate system of the beam. For the "*K th*" layer of an elastic layer composite, the bending stress is defined by Setoodeh and Azizi (2015) as follows

$$\sigma_{Lk} = -z(\bar{Q}_{11})_k \frac{\partial^2 w}{\partial x^2} \tag{3}$$

The equivalent stiffness of the "*K th*" is $(\bar{Q}_{11})_k$, which can be expressed using the classical theory of layered composites as follows by Setoodeh and Azizi (2015)

$$\begin{aligned} (\bar{Q}_{11})_k = {} & Q_{11}\cos^4\theta_k + 2(Q_{12}+2Q_{66})\sin^2\theta_k\cos^2\theta_k \\ & + Q_{22}\sin^4\theta_k \end{aligned} \tag{4}$$

where

$$\begin{aligned} Q_{11} &= \frac{E_1}{1-\nu_{12}\nu_{21}}, \quad Q_{12} = \frac{\nu_{12}E_2}{1-\nu_{12}\nu_{21}}, \\ Q_{22} &= \frac{E_2}{1-\nu_{12}\nu_{21}}, \quad Q_{66} = G_{12} \end{aligned} \tag{5}$$

where "E_1" and "E_2" are the Young's modulus in the longitudinal and transverse directions of the fibers respectively. "ν_{12}" and "ν_{21}" are Poisson's ratios and "θ" is fiber angle.

The stress in PZT layers can be obtained by using the piezoelectric structural equations (Dai *et al*. 2014)

$$\sigma_p = E_p\varepsilon_1^p(x,t) - \bar{e}_{31}E_3(t) \tag{6}$$

In the Eq. (6) "E_p" is Young's modulus of piezoelectric layer, "ε_1^p" is the axial component of strain, "$\bar{e}_{31}$" is piezoelectric constant and "E_3" is electric field in beam thickness.

According to the Euler-Bernoulli beam theory, the result of the torque created in the sandwich beam can be obtained by placing Eqs. (3)-(5) into Eq. (2) as follows

$$M(x,t) = YI\frac{\partial^2 w(x,t)}{\partial x^2} + \Gamma_p v(t)[H(x)-H(x-L)] \tag{7}$$

where "YI" is flexural rigidity equivalent to composite beam, "Γ_p" is electrical coupling coefficient, and "$H(x)$" is unit step function. Because the length of the piezoelectric layers can be equal to the length of the beam or a part of the beam, for this reason, step function in Eq. (7) was used. Also, it is noted that from Fig. 1, the length of the piezoelectric layers is smaller the length of beam, thus step function is defined.

The flexural rigidity of the bimorph beam equivalent can be obtained by using Eqs. (2)-(3) as follows

$$YI = b\sum_{k=1}^{N_c}(\bar{Q}_{11})_k\int_{z_{k-1}}^{z_k} z^2 dz + E_p b\sum_{k=1}^{N_p}\int_{z_{k-1}}^{z_k} z^2 dz \tag{8}$$

Given that there are two piezoelectric layers at the top and bottom surface of the bimorph composite beam, the above relationship can be rewritten as follows

$$\begin{aligned} YI = {} & b\sum_{k=1}^{N_c}(\bar{Q}_{11})_k\int_{z_{k-1}}^{z_k} z^2 dz \\ & + E_p b\left(\int_{-\frac{h_S}{2}-h_p}^{-\frac{h_S}{2}} z^2 dz + \int_{\frac{h_S}{2}}^{\frac{h_S}{2}+h_p} z^2 dz\right) \end{aligned} \tag{9}$$

The amount of electric field in the piezoelectric layer depends on how the voltage is measured from the system. It is possible to place two piezoelectric layers in the electrical circuit in parallel and series. Considering the series circuit, the electrical coupling coefficient is considered as follows by Erturk and Inman (2009)

$$\Gamma_p = \frac{\bar{e}_{31}b}{2h_p}\left[\frac{h_s^2}{4} - \left(h_p+\frac{h_s}{2}\right)^2\right] \tag{10}$$

By substitution Eq. (7) into Eq. (1), the governing equation of the vibrational behavior is obtained as follows

$$\begin{aligned} & YI\frac{\partial^4 w(x,t)}{\partial x^4} + \Gamma_p v(t)\left[\frac{d\delta(x)}{dx} - \frac{d\delta(x-L)}{dx}\right] \\ & + C_sI\frac{\partial^5 w(x,t)}{\partial x^4\partial t} + C_a\frac{\partial w(x,t)}{\partial t} \\ & + (m + M_1\delta(x-L))\frac{\partial^2 w(x,t)}{\partial t^2} = f(x,t) \end{aligned} \tag{11}$$

Also, with respect to the piezoelectric structural equations, another fundamental relation for the calculation "$w(x,t)$" and "$v(t)$" variables is defined as follows by Erturk and Inman (2011)

$$D_3(x,t) = \bar{e}_{31}\sigma_p(x,t) + \varepsilon_{33}E_3(t) \tag{12}$$

where "D_3" and "ε_{33}" are electrical displacement and electrical capacity at constant stress, respectively. Considering the Eq. (12) the amount of "$i(t)$" and "$V(t)$"

can be calculated according to the electric charge "$q(t)$" as follows

$$i(t) = \frac{dq}{dt} = -\int \bar{e}_{31} h_p b \frac{\partial^3 w(x,t)}{\partial x^2 \partial t} dx - \frac{\varepsilon_{33} bL}{h_p} \frac{dV(t)}{dt} \quad (13)$$

$$V(t) = -R\left(\int_0^L \bar{e}_{31} h_p b \frac{\partial^3 w(x,t)}{\partial x^2 \partial t} dx - \frac{\varepsilon_{33} bL}{h_p} \frac{dV(t)}{dt} \right) \quad (14)$$

Using the Eq. (14), it is possible to determine the voltage generated by the piezoelectric layers of the bimorph composite beam. Considering the Eqs. (11)-(14), the "$V(t)$" and "$w(x,t)$" parameters can be determined. Also, by considering the relationship between the voltage and the electric current, Eq. (14) can be expressed in the following standard form

$$\frac{V(t)}{R} + \frac{\varepsilon_{33} bL}{h_p} \frac{dV(t)}{dt} = -\int_0^L \bar{e}_{31} h_p b \frac{\partial^3 w(x,t)}{\partial x^2 \partial t} dx \quad (15)$$

In the present study, the model developed by (Facchinetti *et al*. 2004) is used to investigate the induced vibration behavior of the bimorph composite beam. According to this model, to simulate a fluid oscillator, the nonlinear van der pol equation is used, which has the following relation by Facchinetti *et al*. (2004) as follows

$$\frac{\partial^2 \bar{q}(x,t)}{\partial t^2} + \delta \omega_s [\bar{q}(x,t)^2 - 1] \frac{\partial \bar{q}(x,t)}{\partial t} + \omega_s^2 \bar{q}(x,t) = F_d \quad (16)$$

where "F_d" is the force of fluid that affects on the structure, the dimensionless wake variable "q" may be associated to the fluctuating lift coefficient on the structure, as for most of the models in the literature since the pioneering work of Hartlen and Currie (1970). It may alternatively be considered as a hidden flow variable related to a weighted average of the transverse component of the flow (Blevins and Vibrations 1990). "δ" is the fluid flow damping coefficient which is added. It is usually 0.3 and dependent on the average drag coefficient (Facchinetti *et al*. 2004). "ω_s" is vortex shedding which is as follows (Facchinetti *et al*. 2004)

$$\omega_s = 2\pi S_t \frac{U_e}{D} \quad (17)$$

where "S_t" is the dimensionless number of Strouhal value which is determined by the geometry of the cross-sectional area of the object (Ciappi *et al*. 2015). In this model, the interaction between the fluid and the structure is applied using the force component. The effect of vortex Shedding vibrations introduced by "$\bar{q}(x,t)$" and usually considered proportional to the amplitude. According to the theory presented by Facchinetti *et al*. (2004), the best relation that represents these forces and it is in good agreement with the experimental results is as follows

$$F_d = \frac{P}{D} \frac{\partial^2 w(x,t)}{\partial t^2} \quad (18)$$

which is obtained " $P = 12$ " after processing the experimental data. In Eq. (11), "$f(x,t)$ " is the result of external forces that effected on the bimorph beam. Generally external forces can be divided into two lift force "$f_L(x,t)$", and the damping force "$f_D(x,t)$" that caused by Vortex Shedding. According to studies by Facchinetti *et al*. 2004) and Keber and Wiercigroch (2008), component of forces can be expressed as follows

$$f_D(x,t) = -\frac{1}{2} C_D \rho_f D U_e \frac{\partial w(x,t)}{\partial t} \quad (19a)$$

$$f_L(x,t) = \frac{1}{4} C_L \rho_f D U_e^2 \bar{q}(x,t) \quad (19b)$$

where C_D, C_L, U_e, D, and ρ_f are the damping coefficient, lift coefficient, fluid flow velocity, hydrodynamic diameter and fluid density, respectively. Finally, by considering Eqs. (11)-(14)-(16)-(19) and considering general form of $V(t) = R\frac{dq(t)}{dt}$ the governing equations of the induced vibrational behavior for biomorphic sandwich beam and also the output voltage can be expressed as follows

$$\begin{aligned} &YI \frac{\partial^4 w(x,t)}{\partial x^4} + C_s I \frac{\partial^5 w(x,t)}{\partial x^4 \partial t} + C_a \frac{\partial w(x,t)}{\partial t} \\ &+ \Gamma_p V(t) \left[\frac{d\delta(x)}{dx} - \frac{d\delta(x-L)}{dx} \right] \\ &+ \left(m + M_1 \delta(x-L)\right) \frac{\partial^2 w(x,t)}{\partial t^2} \\ &= \frac{1}{4} C_L \rho_f D U_e^2 \bar{q}(x,t) - \frac{1}{2} C_D \rho_f D U_e \frac{\partial w(x,t)}{\partial t} \end{aligned} \quad (20)$$

$$\frac{\partial^2 \bar{q}(x,t)}{\partial t^2} + \delta \omega_s [\bar{q}(x,t)^2 - 1] \frac{\partial \bar{q}(x,t)}{\partial t} + \omega_s^2 \bar{q}(x,t) = \frac{P}{D} \frac{\partial^2 w(x,t)}{\partial t^2} \quad (21)$$

$$\frac{V(t)}{R} + \frac{\varepsilon_{33} bL}{h_p} \frac{dV(t)}{dt} = -\int_0^L \bar{e}_{31} h_p b \frac{\partial^3 w(x,t)}{\partial x^2 \partial t} dx \quad (22)$$

The dimensionless variables are defined as follows

$$\begin{aligned} &w^* = \frac{w}{D}, \quad x^* = \frac{x}{L}, \quad \tau = \frac{1}{L^2}\sqrt{\frac{YI}{m}}t, \quad c_s = \frac{C_s I}{L^2}\sqrt{\frac{1}{mYI}}, \\ &c_a = C_a L^2 \sqrt{\frac{1}{mYI}}, \quad \Gamma_p^* = \frac{\Gamma_p L^3}{YID} \\ &\beta = \frac{M_1}{m}, \quad u = \sqrt{\frac{m}{YI}} L U_e, \quad c_L = \frac{C_L \rho_f L^2}{4m}, \\ &c_D = \frac{C_D \rho_f LD}{2m}, \quad \lambda = 2\pi S_t \frac{L}{D} \\ &\mu_0 = \frac{\varepsilon_{33} bR}{h_p L}\sqrt{\frac{YI}{m}}, \quad \mu_1 = \frac{\bar{e}_{31} h_p bRD}{L}\sqrt{\frac{YI}{m}} \end{aligned} \quad (23)$$

The governing equations of sandwich beam under external and internal damping can be expressed in terms of dimensionless parameters as follows

$$\frac{\partial^4 w^*(x^*,\tau)}{\partial x^{*4}} + c_s \frac{\partial^5 w^*(x^*,\tau)}{\partial x^4 \partial \tau} + c_a \frac{\partial w^*(x^*,\tau)}{\partial \tau} + \Gamma_p^* V(\tau)\left[\frac{d\delta(x^*)}{dx^*} - \frac{d\delta(x^*-1)}{dx^*}\right] + \left(1+\beta\delta(x^*-1)\right)\frac{\partial^2 w^*(x^*,\tau)}{\partial \tau^2} = c_L u^2 \bar{q}(x^*,\tau) - c_D u \frac{\partial w^*(x^*,\tau)}{\partial \tau} \quad (24)$$

$$\frac{\partial^2 \bar{q}(x^*,\tau)}{\partial \tau^2} + \delta\lambda u[\bar{q}(x^*,\tau)^2 - 1]\frac{\partial \bar{q}(x^*,\tau)}{\partial \tau} + \lambda^2 u^2 \bar{q}(x^*,\tau) = P\frac{\partial^2 w^*(x^*,\tau)}{\partial \tau^2} \quad (25)$$

$$V(t) + \mu_0 \frac{dV(t)}{dt} = -\mu_1 \int_0^1 \frac{\partial^3 w(x^*,\tau)}{\partial x^{*2} \partial \tau} dx^* \quad (26)$$

We will ignore superscript »∗« in the following for reducing of overwriting. The Galerkin method is used to solve the nonlinear coupling differential equations. Accordingly, the hypothetical answer to the equation of motion is assumed as follows

$$w(x,\tau) = \sum_{r=1}^{N} \phi_r(x)\eta_r(\tau) \quad (27)$$

$$\bar{q}(x,\tau) = \sum_{r=1}^{N} \phi_r(x) q_r(\tau) \quad (28)$$

where "$\phi_r(x)$" is normalized mode shape of cantilever bream, "$\eta_r(\tau)$" and "$q_r(\tau)$" are the generalized coordinates correspond to the "*r th*" modes. Considering the boundary conditions, the comparison function can be expressed as follows by Rao (2007)

$$\phi(x) = cosh(\alpha_n x) - cos(\alpha_n x) - \frac{cosh(\alpha_n) + cos(\alpha_n)}{sinh(\alpha_n) + sin(\alpha_n)}(sinh(\alpha_n x) - sin(\alpha_n x)) \quad (29)$$

where eigenvalues of "α_n" solve by following equation

$$cos\,\alpha_n\, cosh\,\alpha_n = -1 \quad (30)$$

By substitution Eq. (24) into Eq. (23), we will have

$$V(\tau) + \mu_0 \frac{dV(\tau)}{d\tau} = -\mu_1 \sum_{n=1}^{N} P_n \frac{d\eta_n(\tau)}{d\tau} \quad (31)$$

Eq. (31) can be solved by multiplying the integral factor ($\mu = e^{\frac{\tau}{\tau_c}}$). "$\tau_c$" is time constant of electric circuit which is defined ($\tau_c = \frac{1}{\mu_0}$). In this case, the answer to the differential Eq. (31) is as follows

$$V(\tau) = -e^{-\frac{\tau}{\tau_c}}\left[\int e^{\frac{\tau}{\tau_c}} \sum_{n=1}^{N} \mu_1 P_n \frac{d\eta_n(\tau)}{d\tau} d\tau + C_0\right] \quad (32)$$

Assuming an initial voltage of zero, we will have

$$V(\tau) = -\mu_1 e^{-\frac{\tau}{\tau_c}} \sum_{n=1}^{N} \left(\int e^{\frac{\tau}{\tau_c}} \frac{d\eta_n(\tau)}{d\tau} d\tau\right) \quad (33)$$

By substitution Eq. (33) into Eq. (24) and using Eqs. (27)-(28) and applying the Galerkin method, Eqs. (24)-(25) appear as ordinary derivative differential equations solving the "$\eta_n(\tau)$"and "$q_n(\tau)$". Finally, the influence of different parameters has been studied.

3. Result and discussion

In this section, the results of solving the equations for energy harvesting from a rectangular sandwich beam with piezoelectric face sheets are presented. Laminated composite is made of Glass fiber/epoxy and also the piezoelectric layers are ceramic type *PZT5A*. The mechanical properties and geometrical dimensions of the model are shown in Tables 1 to 3. The mechanical properties of the used E-glass fiber / Epoxy composite in the rectangular beam are shown in Table 2 (Kathiresan *et al*. 2012). External fluid is considered water and the coefficients values "C_D", "C_L" and "S_t" are used from the reference Blevins (1977). The coefficients of oscillations "δ" and "P" of the values presented are used in the reference (Yamamoto *et al*. 2004). The differential equations with the obtained ordinary derivative by using the Runge-Kutta method and the response to these equations is obtained for different values of the system parameters. In deriving the results it is assumed that the beam is affected by the initial pure displacement conditions and it vibrates as $q_i = \eta_i = 0.001,\ \dot{q}_i = \dot{\eta}_i = 0.0$.

To validate the accuracy of the results in the present study, the results are compared with a research which is done by Zarepour (2017) and Yamamoto *et al*. (2004). They used a semi-analytical method, and investigated the behavior of induced vibrations in a beam with a rectangular cross section under the influence of external fluid flow. For comparison between the results of the present study and the reference results Zarepour (2017), the boundary conditions and the geometrical characteristics used are similar to the

Table 1 Geometrical dimensions of bimorph rectangular composite beam

L	B	h_s	h_p
500 mm	20 mm	2 mm	0.1 mm

Table 2 E-glass fiber/epoxy composite properties

E_1	E_2	G_{12}	v_{12}	v_{21}	ρ
130.90 GPa	8.30 GPa	2.80 GPa	0.0866	0.0866	1800 kg/m^3

Table 3 Mechanical properties of piezoelectric layers

E_p	d_{31}	ε_{33}	e_{31}	ρ_p
130.90 GPa	8.30 GPa	2.80 GPa	0.0866	0.0866

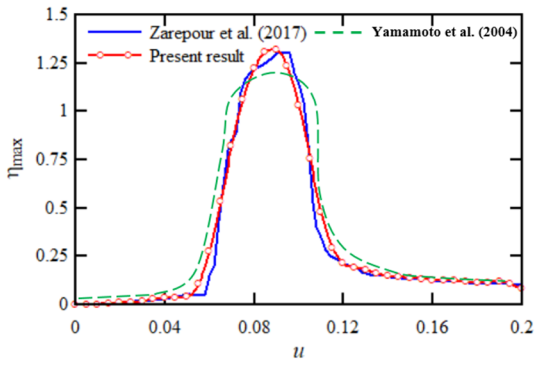

Fig. 2 Comparison of the maximum amplitude variation curve in terms of fluid velocity obtained from the present study and the reference results

specifications presented in the reference. Fig. 2 compares the maximum amplitude change curve in terms of fluid velocity that is obtained from the results of the present study and the literature results including Yamamoto *et al.* (2004) and Zarepour (2017). As the results show, the presentation method accurately predicts the vibration behavior of the beams under the influence of external fluid flow.

In the following, the effect of different parameters on the energy harvesting of the bimorph sandwich beam is investigated. In Fig. 3, the midpoint response and the voltage produced by the piezoelectric layers for different external fluid velocities $u = 0.0$, $u = 0.1$ and $u = 0.38$ for two different layers of [45, -45, -45, 45] and [0, 0, 0, 0] have been shown. Since the governing equations are solved in terms of dimensionless variables, therefore, the flexural strength changes would not have an equivalent effect on the frequency of the dimensional oscillations of the bimorph composite beam but its effect on the amplitude response and output voltage will be noticeable. According to Fig. 3(a), it is observed that in the absence of external fluid flow the system response is oscillatory damping. In this case, only the effect of the added mass due to the fluid is affected, which reduces the natural frequency of the beam. With increasing fluid velocity and at low fluid velocities corresponding to very small Reynolds and Strouhal numbers, the fluid flow around the beam is very slow or creepy. As the fluid flows around the beam, von Kármán vortex shedding is symmetrically created by negative pressure on the back of the beam, causing lift and drag forces on the beam, as a result, they cause vibrations in the beam. Also, the results show that the angle of the composite beam fibers has a significant effect on the maximum oscillation amplitude and the amount of energy harvested. On the basis of the presented results, we can see in Fig. 2(b) the energy harvesting of layers [0, 0, 0, 0] are more than [45, -45, -45, 45]. For example, layers of [0, 0, 0, 0] for non-dimensional velocities of 0.1 and 0.38, it increases about 25 and 27% at the maximum harvested voltage relative to the corresponding state [45, -45, -45, 45]. Structural and fluid interaction occurs as a result of the transfer of lift forces from the fluid to the beam, which is highly dependent on the fluid velocity. As shown in the results, the fluid velocity changes the vibrational behavior of the system. As shown in Fig. 3(c), it is observed that, for a dimensionless velocity of 0.38, the amplitude of the oscillation increases over time and eventually converges to a constant value. In this case, especially the von Kármán vortex are symmetrically created by negative pressure on the back of the beam, causing lift forces on the beam, thereby increasing the amplitude of the vibrations.

Fig. 4 shows the variation of the maximum amplitude of the oscillations in terms of fluid velocity for the two different layers [45, -45, -45, 45] and [0, 0, 0, 0]. As can be seen at low fluid velocities, the fluid flow around the beam causes the system's response to be oscillatory damping. Over time, the amplitude of the fluctuations tends to zero. As the flow velocity and the Reynolds number increases, the vortex area of the beam expands and the drag force has a dominant effect on the total refractive force and vibration of the beam. This is because at low speeds this force causes the amplitude of vibrations to dampen. As fluid velocity increases further, fluid inertia forces have a significant effect on the response of the system. This causes the system's vibration amplitude to increase abruptly at higher

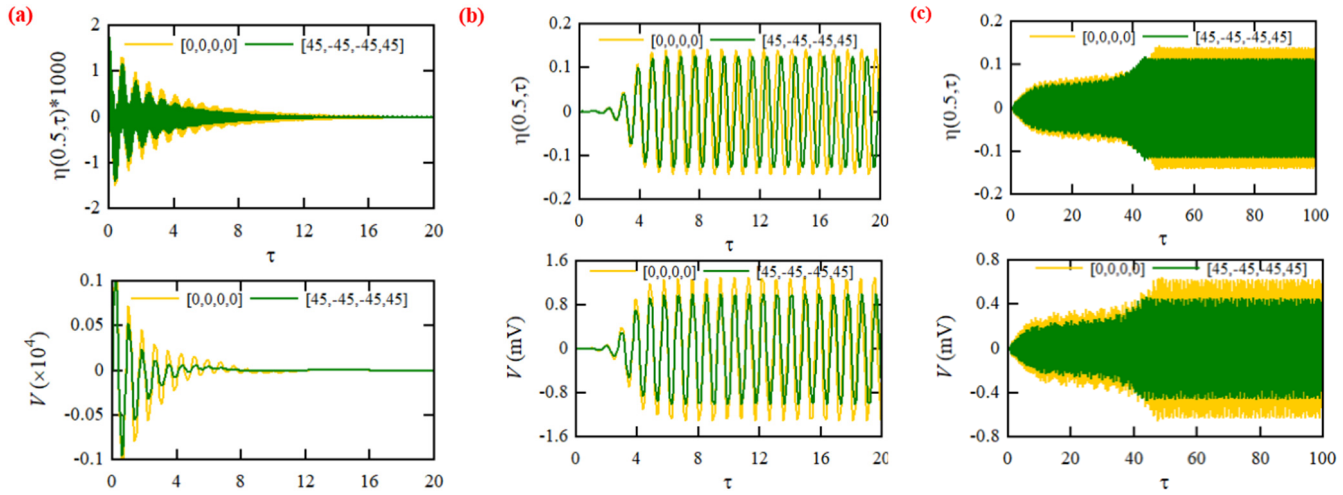

Fig. 3 Midpoint response and voltage generation by piezoelectric layers for different dimensions of external Fluid flow (a) $u = 0$; (b) $u = 0.1$; (c) $u = 0.38$

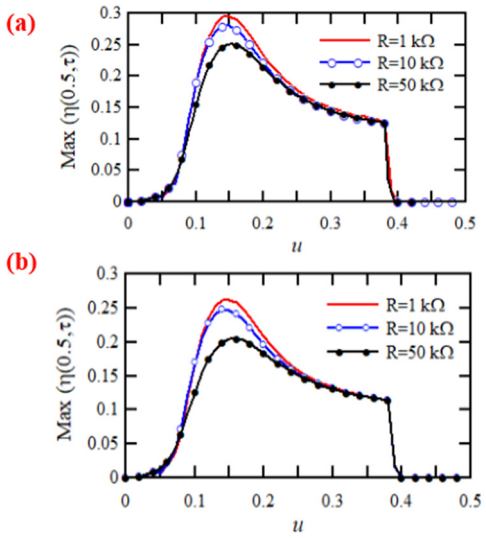

Fig. 4 Changes of maximum amplitude of oscillations in terms of fluid velocity: (a) Layer [0, 0, 0, 0]; (b) Layer [45, -45, -45, 45]

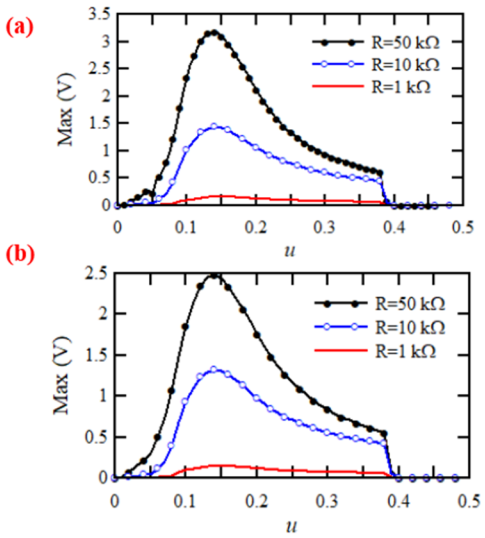

Fig. 5 Maximum voltage variations produced by fluid velocity: (a) Layer [0, 0, 0, 0]; (b) Layer [45, -45, -45, 45]

speeds and the behavior of the system to be oscillatory. This range of fluid velocity is called the locking zone. In the post-lock zone, a further increase in fluid velocity reduces the amplitude of the oscillation and the steady-state amplitude of the system reaches zero. Within this range, fluid-resisting forces override the inertia and return forces of the beam and cause the beam to settle. As can be seen from the results, the steady-state vibration amplitude for the locking area is greater than the other two areas. Another result that can be seen in Fig. 4 is that the amount of electrical resistivity of the energy harvesting circuit also affects the maximum amplitude of the system oscillations and by increasing its value, the maximum amplitude of the oscillating bimorph beam understudy is reduced. Such a similar behavior can be observed for the maximum value of voltage produced using Fig. 5. As can be seen from the figure, in the locked areas due to the higher amplitude of the oscillations, the amount of voltage produced is higher than in other areas. It is also observed when the electrical resistance increases, the maximum voltage produced also increases and this increase is highly dependent on the layout of the composite beam layers. For example, for u = 0.15 by increasing the electrical resistance of the circuit from 1 kΩ to 50 kΩ the maximum voltage for layering [45, -45, -45, 45] and [0, 0, 0, 0], increases about 94% and 96% respectively. Also, the results show that the layering arrangement and the electrical resistance value of the circuit

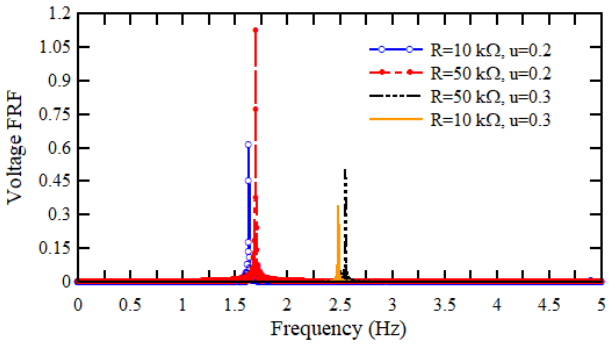

Fig. 6 The voltage response function of the harvested voltage each layer [0, 0, 0, 0]

did not have a significant effect on the locking area and for the bimorph composite beam under the maximum amplitude of the oscillations as well as the maximum voltage produced at a velocity of 0.15.

Fig. 6 shows the frequency response function of the voltage applied to the layer [0, 0, 0, 0] and different fluid velocities. The results show that the frequency corresponding to the maximum energy harvesting is in addition to the electrical resistivity of the fluid flow rate. The results show that for a given fluid velocity, the resonant frequency corresponding to the maximum voltage produced

Table 4 Comparison of the maximum voltage of four-layer composite beam $[\theta, -\theta, -\theta, \theta]$ with different values of the layer fiber angle

u	θ								
	0	10	20	30	40	50	60	80	90
0.10	2.26	2.14	2.13	2.03	2.02	2.01	2.02	2.25	2.33
0.15	3.15	3.00	2.84	2.64	2.63	2.62	2.65	3.01	3.07
0.20	2.14	2.12	2.00	1.94	1.93	1.91	1.93	2.02	2.13
0.25	1.32	1.30	1.30	1.28	1.27	1.26	1.28	1.31	1.31

decreases with increasing resistance value.

The results show that the angle of the fibers has a significant effect on the structural damping coefficient, flexural stiffness, natural frequency and ultimately energy harvesting. Table 4 shows the effect of fiber angle on the maximum voltage and shown for different fluid velocities. In this table, the layers are presented as $[\theta, -\theta, -\theta, \theta]$, and the results are presented for different values of angle "θ". The minimum voltage is for using the fibers with 50 degrees, and the maximum voltage is for using the fibers with zero degrees. This is due to the dependence of the modulus of elasticity of the composite beam on the fiber angle and its attenuation coefficient. Since the bending stiffness of the layer is zero degrees higher and its damping coefficient is lower, so the energy harvesting rate will be highest in this case.

4. Conclusions

In this paper, an analytical method was developed to determine the amount of energy harvesting from a piezoelectric composite beam under induced vibrations and also the effect of various parameters on the rate of energy harvesting was studied. The angle of orientation of the fibers and the layout of layers has a significant effect on the energy harvesting. It can be seen from the results that if the layout of the layers and their fiber angles are such that the amount of modulus of elasticity equivalent to the load is reduced, then the natural frequency and energy harvesting from the system will be reduced. In other words, the energy harvesting can be greatly improved by using zero-degree layers. Increasing the electrical resistance increases the output voltage and consequently decreases the current passing through the circuit. By observing the results presented for bimorph composite beam, the output voltage of the circuit has almost doubled as the electrical resistance increases from 1000 to 5000 kHz.

Acknowledgments

The authors would like to thank the referees for their valuable comments. Also, they are thankful to the Iranian Nanotechnology Development Committee for their financial support and the University of Kashan for supporting this work.

Declaration of Competing Interest

No conflict of interest exists in the submission of this article, and the article is approved by all authors for publication.

References

AkhavanAlavi, S.M., Mohammadimehr, M. and Edjtahed, S.H. (2019), "Active control of micro Reddy beam integrated with functionally graded nanocomposite sensor and actuator based on linear quadratic regulator method", *Eur. J. Mech.-A/Solids*, **74**, 449-461. https://doi.org/10.1016/j.euromechsol.2018.12.008

Alsaadi, A., Shi, Y., Pan, L., Tao, J. and Jia, Y. (2019). "Vibration energy harvesting of multifunctional carbon fibre composite laminate structures", *Compos. Sci. Technol.*, **178**, 1-10. https://doi.org/10.1016/j.compscitech.2019.04.020

An Tan, C., Amoozegar, S. and Lai, H.L. (2018), "Transfer function analysis of constrained, distributed piezoelectric vibration energy harvesting beam systems", *J. Vib. Acoust.*, **140**(3). https://doi.org/10.1115/1.4038949

Babaeeian, M. and Mohammadimehr, M. (2020), "Investigation of the time elapsed effect on residual stress measurement in a composite plate by DIC method", *Optics Lasers Eng.*, **128**, 106002. https://doi.org/10.1016/j.optlaseng.2020.106002

Blevins, R.D. (1977), *Flow-induced vibration*, New York, Van Nostrand Reinhold Co., 377 p.

Blevins, R.D. and Vibrations, F.I. (1990), *Van Nostrand Reinhold*, New York, pp. 104-110.

Cahill, P., Pakrashi, V. and Sun, P. (2018), "Energy harvesting techniques for health monitoring and indicators for control of a damaged pipe structure", *Smart Struct. Syst., Int. J.*, **21**(3), 287-303. https://doi.org/10.12989/sss.2018.21.3.287

Ciappi, E., De Rosa, S., Franco, F., Guyader, J.L. and Hambric, S.A. (2015), *Flinovia-Flow Induced Noise and Vibration Issues and Aspects*, New York, Springer, pp. 67-115.

Dai, H.L., Abdelkefi, A. and Wang, L. (2014), "Piezoelectric energy harvesting from concurrent vortex-induced vibrations and base excitations", *Nonlinear Dyn.*, **77**(3), 967-981. https://doi.org/10.1007/s11071-014-1355-8

Erturk, A. and Inman, D.J. (2009), "An experimentally validated bimorph cantilever model for piezoelectric energy harvesting from base excitations", *Smart Mater. Struct.*, **18**(2), 025009. https://doi.org/10.1088/0964-1726/18/2/025009

Erturk, A. and Inman, D.J. (2011), *Piezoelectric Energy Harvesting*, John Wiley & Sons, UK. https://doi.org/10.1002/9781119991151

Facchinetti, M.L., De Langre, E. and Biolley, F. (2004), "Coupling of structure and wake oscillators in vortex-induced vibrations", *J. Fluids Struct.*, **19**(2), 123-140. https://doi.org/10.1016/j.jfluidstructs.2003.12.004

Farazin, A. and Mohammadimehr, M. (2020), "Nano research for investigating the effect of SWCNTs dimensions on the properties of the simulated nanocomposites: a molecular dynamics simulation", *Adv. Nano Res., Int. J.*, **9**(2), 83-90. https://doi.org/10.12989/anr.2020.9.2.083

Farazin, A., Aghdam, H.A., Motififard, M., Aghadavoudi, F., Kordjamshidi, A., Saber-Samandari, S. and Khandan, A. (2019), "A polycaprolactone bio-nanocomposite bone substitute fabricated for femoral fracture approaches: Molecular dynamic and micro-mechanical Investigation", *J. Nanoanal.*, **6**(3), 172-184. https://doi.org/10.22034/jna.2019.584848.1134

Farazin, A., Aghadavoudi, F., Motififard, M., Saber-Samandari, S. and Khandan, A. (2020), "Nanostructure, molecular dynamics simulation and mechanical performance of PCL membranes reinforced with antibacterial nanoparticles", *J. Appl. Computat. Mech.*, **7**(2). https://doi.org/10.22055/JACM.2020.32902.2097

Ghorbanpour Arani, A. and Zamani, M.H. (2018), "Nonlocal free vibration analysis of FG-porous shear and normal deformable sandwich nanoplate with piezoelectric face sheets resting on silica aerogel foundation", *Arab. J. Sci. Eng.*, **43**(9), 4675-4688. https://doi.org/10.1007/s13369-017-3035-8

Ghorbanpour Arani, A., Mosayyebi, M., Kolahdouzan, F., Kolahchi, R. and Jamali, M. (2017), "Refined zigzag theory for vibration analysis of viscoelastic functionally graded carbon nanotube reinforced composite microplates integrated with piezoelectric layers", *Proceedings of the Institution of Mechanical Engineers, Part G: Journal of Aerospace Engineering*, **231**(13), 2464-2478.

https://doi.org/10.1177/0954410016667150

Ghorbanpour Arani, A., Rousta Navi, B., Mohammadimehr, M., Niknejad, S., Ghorbanpour Arani, A.A. and Hosseinpour, A. (2019), "Pull-in instability of MSGT piezoelectric polymeric FG-SWCNTs reinforced nanocomposite considering surface stress effect", *J. Solid Mech*., **11**(4), 759-777. https://doi.org/10.22034/JSM.2019.668611

Hannan, M.A., Hassan, K. and Jern, K.P. (2018), "A review on sensors and systems in structural health monitoring: Current issues and challenges", *Smart Struct. Syst*., *Int. J*., **22**(5), 509-525. https://doi.org/10.12989/sss.2018.22.5.509

Hartlen, R.T. and Currie, I.G. (1970), "Lift-oscillator model of vortex-induced vibration", *J. Eng. Mech. Div*., **96**(5), 577-591. https://doi.org/10.1061/JMCEA3.0001276

Kathiresan, M., Manisekar, K. and Manikandan, V. (2012), "Performance analysis of fiber metal laminated thin conical frusta under axial compression", *Compos. Struct*., **94**(12), 3510-3519. https://doi.org/10.1016/j.compstruct.2012.05.026

Keber, M. and Wiercigroch, M. (2008), "Dynamics of a vertical riser with weak structural nonlinearity excited by wakes", *J. Sound Vib*., **315**(3), 685-699. https://doi.org/10.1016/j.jsv.2008.03.023

Kim, J., Swartz, A., Lynch, J.P., Lee, J.J. and Lee, C.G. (2010), "Rapid-to-deploy reconfigurable wireless structural monitoring systems using extended-range wireless sensors", *Smart Struct. Syst*., *Int. J*., **6**(5-6), 505-524. https://doi.org/10.12989/sss.2010.6.5_6.505

Kim, J.M., Han, M., Lim, H.J., Yang, S. and Sohn, H. (2016), "Operation of battery-less and wireless sensor using magnetic resonance based wireless power transfer through concrete", *Smart Struct. Syst*., *Int. J*., **17**(4), 631-646. https://doi.org/10.12989/sss.2016.17.4.631

Khandan, A., Saber-Samandari, S., Telloo, M., Kazeroni, Z.S., Esmaeili, S., Sheikhbahaei, E. and Kamyab, B. (2020), "A mitral heart valve prototype using sustainable polyurethane polymer: fabricated by 3D bioprinter, tested by molecular dynamics simulation", *AUT J. Mech. Eng*. https://doi.org/10.22060/AJME.2020.17450.5862

Li, W., Liu, T.S. and Hsiao, C.C. (2011), "A miniature generator using piezoelectric bender with elastic base", *Mechatronics*, **21**(7), 1183-1189. https://doi.org/10.1016/j.mechatronics.2011.07.004

Li, H., Liu, D., Wang, J., Shang, X. and Hajj, M.R. (2020), "Broadband bimorph piezoelectric energy harvesting by exploiting bending-torsion of L-shaped structure", *Energy Convers. Manage*., **206**, 112503. https://doi.org/10.1016/j.enconman.2020.112503

Mohammadimehr, M., Mohammadimehr, M.A. and Dashti, P. (2016), "Size-dependent effect on biaxial and shear nonlinear buckling analysis of nonlocal isotropic and orthotropic micro-plate based on surface stress and modified couple stress theories using differential quadrature methods", *Appl. Mathe. Mech*., **37**(4), 529-554. https://doi.org/10.1007/s10483-016-2045-9

Mohammadimehr, M., Navi, B.R. and Ghorbanpour Arani, A. (2017), "Dynamic stability of modified strain gradient theory sinusoidal viscoelastic piezoelectric polymeric functionally graded single-walled carbon nanotubes reinforced nanocomposite plate considering surface stress and agglomeration effects under hydro-thermo-electro-magneto-mechanical loadings", *Mech. Adv. Mater. Struct*., **24**(16), 1325-1342. https://doi.org/10.1080/15376494.2016.1227507

Mohammadimehr, M., Mohammadi-Dehabadi, A.A., AkhavanAlavi, S.M., Alambeigi, K., Bamdad, M., Yazdani, R. and Hanifehlou, S. (2018), "Bending, buckling, and free vibration analyses of carbon nanotube reinforced composite beams and experimental tensile test to obtain the mechanical properties of nanocomposite", *Steel Compos. Struct*., *Int. J*., **29**(3), 405-422. https://doi.org/10.12989/scs.2018.29.3.405

Ottman, G.K., Hofmann, H.F., Bhatt, A.C. and Lesieutre, G.A. (2002), "Adaptive piezoelectric energy harvesting circuit for wireless remote power supply", *IEEE Transact. Power Electron*., **17**(5), 669-676. https://doi.org/10.1109/TPEL.2002.802194

Rajabi, J. and Mohammadimehr, M. (2019), "Bending analysis of a micro sandwich skew plate using extended Kantorovich method based on Eshelby-Mori-Tanaka approach", *Comput. Concrete*, *Int. J*., **23**(5), 361-376. https://doi.org/10.12989/cac.2019.23.5.361

Rao, S.S. (2007), *Vibration of Continuous Systems*, New York: Wiley, Vol. 464.

Setoodeh, A.R. and Azizi, A. (2015), "Bending and free vibration analyses of rectangular laminated composite plates resting on elastic foundation using a refined shear deformation theory", *Iran. J. Mater. Form*., **2**(2), 1-13. https://doi.org/10.22099/IJMF.2015.3236

Shan, X., Li, H., Yang, Y., Feng, J., Wang, Y. and Xie, T. (2019), "Enhancing the performance of an underwater piezoelectric energy harvester based on flow-induced vibration", *Energy*, **172**, 134-140. https://doi.org/10.1016/j.energy.2019.01.120

Soleymani, T. and Ghorbanpour Arani, A. (2019), "On aeroelastic stability of a piezo-MRE sandwich plate in supersonic airflow", *Compos. Struct*., **230**, 111532. https://doi.org/10.1016/j.compstruct.2019.111532

Trentadue, F., Quaranta, G., Maruccio, C. and Marano, G.C. (2019), "Energy harvesting from piezoelectric strips attached to systems under random vibrations", *Smart Struct. Syst*., *Int. J*., **24**(3), 333-343. https://doi.org/10.12989/sss.2019.24.3.333

Umeda, M., Nakamura, K. and Ueha, S. (1996), "Analysis of the transformation of mechanical impact energy to electric energy using piezoelectric vibrator", *Japanese J. Appl. Phys*., **35**(5S), 3267. https://doi.org/10.1143/JJAP.35.3267

Xie, J., Yang, J., Hu, H., Hu, Y. and Chen, X. (2012), "A piezoelectric energy harvester based on flow-induced flexural vibration of a circular cylinder", *J. Intell. Mater. Syst. Struct*., **23**(2), 135-139. https://doi.org/10.1177/1045389X11431744

Yamamoto, C.T., Meneghini, J.R., Saltara, F., Fregonesi, R.D.A. and Ferrari Jr, J.A. (2004), "Numerical simulations of vortex-induced vibration on flexible cylinders", *J. Fluids Struct*., **19**(4), 467-489. https://doi.org/10.1016/j.jfluidstructs.2004.01.004

Zarepour, G.R. (2017), "Vortex Induced Vibration of Simply Supported Visco elastic Beam", *Modares Mech. Eng*., **17**(9), 309-318.

Zhou, S., Hobeck, J.D., Cao, J. and Inman, D.J. (2017), "Analytical and experimental investigation of flexible longitudinal zigzag structures for enhanced multi-directional energy harvesting", *Smart Mater. Struct*., **26**(3), 035008. https://doi.org/10.1088/1361-665X/26/3/035008.

CC

Appendix A

The displacement fields for Euler-Bernoulli beam model are written as follows

$$\begin{aligned} u(x,y,z,t) &= -z\frac{\partial w(x,t)}{\partial x} \\ v(x,y,z,t) &= 0 \\ W(x,y,z,t) &= w(x,t) \end{aligned} \tag{A1}$$

where $u(x,y,z,t)$, $v(x,y,z,t)$, $W(x,y,z,t)$ are the displacements in x, y, z directions, respectively.

The normal strain in x direction is considered as follows

$$\varepsilon_x = -z\frac{\partial^2 w(x,t)}{\partial x^2} \tag{A2}$$

The variation of strain energy for Euler-Bernoulli beam model is illustrated as

$$\delta U = \int_V \sigma_x\, \delta\varepsilon_x dV + \int_V S_x\, \delta\dot{\varepsilon}_x dV \tag{A3}$$

where σ_x and ε_x are the normal stress and strain, respectively. Also, S_x and $\dot{\varepsilon}_x$ depict the stress and strain rates, respectively.

Substituting Eq. (A2) into Eq. (A3) yields the following equation

$$\begin{aligned} \delta U = &\int_V \sigma_x\, \delta(-zw(x,t),xx)dV \\ &+ \int_V S_x\, \delta(-zw(x,t),xxt)dV \end{aligned} \tag{A4}$$

The following equations are defined as

$$\begin{aligned} M(x,t) &= -\int \sigma_x\, z dz \\ M_2(x,t) &= -\int_V S_x\, z dz \end{aligned} \tag{A5}$$

where $M(x,t)$ and $M_2(x,t)$ are the bending moment of beam.

Substituting Eq. (A5) into Eq. (A4) yields

$$\begin{aligned} \delta U = &\int_A M(x,t)\, \delta w(x,t),xx dA \\ &+ \int_V M_2(x,t)\, \delta w(x,t),xxt dV \end{aligned} \tag{A6}$$

Thus, after simplifying, we have

$$\begin{aligned} \delta U = &\int_A \frac{\partial^2 M(x,t)}{\partial x^2}\delta w(x,t)dA \\ &+ \int_A \frac{\partial^3 M_2(x,t)}{\partial x^2 \partial t}\delta w(x,t)dA \end{aligned} \tag{A7}$$

where $M_2(x,t)$ is equal to $\frac{\partial^2}{\partial x^2}(C_s I w(x,t))$. Also, "$C_s$" is the strain-rate damping coefficient (it appears as an effective term "$C_s I$" for the composite structure).

The variation of kinetic energy is defined as follows

$$\delta T = \int_A (\rho\dot{u}\delta\dot{u} + \rho\dot{w}\delta\dot{w})dV + \int_A M_1\, \delta(x-L)w(x,t),t\delta w(x,t),tdA \tag{A8}$$

Substituting Eq. (A1) into Eq. (A8) yields the following equation

$$\begin{aligned} \delta T = &\int_V (\rho\dot{u}\delta\dot{u} + \rho\dot{w}\delta\dot{w})dV \\ &+ \int_A M_1\, \delta(x-L)w(x,t),t\delta w(x,t),tdA \end{aligned} \tag{A9}$$

where "M_1" is the concentrated mass and, "ρ" is the density of beam.

Substituting Eq. (A1) into Eq. (A9) yields the following equations

$$\begin{aligned} \delta T = &\int_V (\rho(-zw,xt)\delta(-zw,xt) + \rho w,t\delta w,t)dV \\ &+ \int_A M_1\, \delta(x-L)w(x,t),t\delta w(x,t),tdA \end{aligned} \tag{A10}$$

The mass moment inertia is considered as

$$\begin{aligned} I^{(2)} &= \int \rho z^2\, dz \\ m &= \int \rho\, dz \end{aligned} \tag{A11}$$

Substituting Eq. (A11) into Eq. (A10) yields

$$\begin{aligned} \delta T = &\int_A I^{(2)}w,xt\delta w,xt + mw,t\delta w,t)dA \\ &+ \int_A M_1\, \delta(x-L)w(x,t),t\delta w(x,t),tdA \end{aligned} \tag{A12}$$

In this research, the term $I^{(2)}w,xt\delta w,xt$ is ignored. Also, "m" is mass of unit length of beam.

After simplifying, we have

$$\begin{aligned} \delta T = &-\int_A m\frac{\partial^2 w(x,t)}{\partial t^2}\delta w dA \\ &-\int_A M_1\, \delta(x-L)\frac{\partial^2 w(x,t)}{\partial t^2}\delta w dA \end{aligned} \tag{A13}$$

The work done by the external work has been considered as

$$\begin{aligned} \delta W_{ext} &= \int_A F_{ext}\delta w dA \\ F_{ext} &= -C_a\frac{\partial w}{\partial t} + f(x,t) \end{aligned} \tag{A14}$$

The principle of the minimum potential energy is defined as

$$\delta\prod = \int_A ((\delta U - \delta W_{ext}) - \delta T)dt = 0 \tag{A15}$$

Substituting Eqs. (A7), (A13) and (A4) into Eq. (A15), the governing equation of motion is obtained as follows

$$\begin{aligned} &\frac{\partial^2 M(x,t)}{\partial x^2} + \frac{\partial^2}{\partial x^2}\left(C_s I\frac{\partial^3 w(x,t)}{\partial x^2 \partial t}\right) + C_a\frac{\partial w(x,t)}{\partial t} \\ &+(m + M_1\delta(x-L))\frac{\partial^2 w(x,t)}{\partial t^2} = f(x,t) \end{aligned} \tag{A16}$$